

Compressibility of the $\text{HgBa}_2\text{Ca}_{n-1}\text{Cu}_n\text{O}_{2n+2+\delta}$ ($n = 1, 2, 3$) high-temperature superconductors

J. H. Eggert, J. Z. Hu, and H. K. Mao

*Carnegie Institution of Washington, Geophysical Laboratory and Center for High Pressure Research,
5251 Broad Branch Rd. N.W., Washington, D.C. 20015-1305*

L. Beauvais, R. L. Meng, and C. W. Chu

Department of Physics and Texas Center for Superconductivity, University of Houston, Houston, Texas 77204

(Received 21 January 1994; revised manuscript received 22 February 1994)

The transition temperatures (T_c) of the homologous series $\text{HgBa}_2\text{Ca}_{n-1}\text{Cu}_n\text{O}_{2n+2+\delta}$ of high-temperature superconductors show very large (~ 30 K) pressure enhancements, saturating at 118, 154, and 164 K for Hg1201, Hg1212, and Hg1223, respectively. We have measured the compressibility of the first three mercury superconductors in a diamond-anvil cell using energy-dispersive synchrotron x-ray diffraction. We report the tetragonal-cell parameters a and c up to 30 GPa. We find ambient-pressure bulk moduli, $K_{V_0} \equiv -V_0(\partial P/\partial V)_0$, of 65.4(3.0), 91.6(4.7), and 83.8(10.5) GPa for Hg1201, Hg1212, and Hg1223, respectively. The Hg superconductors are highly compressible compared to other high-temperature superconductors which generally show bulk moduli in the range of 100–200 GPa. The relation $c = A + B(n-1)$ holds for the c -axis cell parameter at ambient pressure, however, the relation breaks down at high pressures.

Superconductivity at 94, 128, and 135 K was recently reported for optimally doped samples of the homologous series $\text{HgBa}_2\text{Ca}_{n-1}\text{Cu}_n\text{O}_{2n+2+\delta}$ with $n = 1, 2, 3$, respectively.^{1,2} The pressure dependence of T_c for each compound was initially measured to 1–2 GPa Refs. (3–6) and soon thereafter to 15 and 22 GPa for Hg1212,⁷ and Hg1223.^{8,9} These pressure studies all showed a remarkably large pressure enhancement of T_c without saturation. Higher-pressure measurements have now been obtained up to 40 GPa showing saturation of T_c at 118, 154, and 164 K for Hg1201, Hg1212, and Hg1223, respectively.¹⁰ Hg1223 at 30 GPa is the highest temperature superconductor currently known. In addition, it was pointed out¹⁰ that the pressure enhancement of T_c was larger than could be explained by current models.

To understand the high-pressure behavior of these superconductors it is necessary to know the compressibility and the equation of state of each member of the series. Thus, we have measured the unit-cell parameters of Hg1201, Hg1212, and Hg1223 at 300 K in a diamond-anvil cell with a neon pressure medium by energy-dispersive synchrotron x-ray diffraction up to 30 GPa. The interplane compressibility ($\parallel c$) is larger than the intraplane compressibility ($\perp c$) for all three samples. We have extrapolated our high-pressure data to obtain ambient-pressure bulk moduli [$K_{V_0} \equiv -V_0(\partial P/\partial V)_0$] of 65.4(3.0), 91.6(4.7), and 83.8(10.5) GPa for Hg1201, Hg1212, and Hg1223, respectively. The Hg superconductors are highly compressible compared to other high-temperature superconductors which generally show bulk moduli in the 100–200 GPa range.¹¹

The preparation of $\text{HgBa}_2\text{Ca}_{n-1}\text{Cu}_n\text{O}_{2n+2+\delta}$ samples has been discussed many times previously^{8,12} so only a brief summary will be given here. The samples were prepared using the controlled vapor-solid reaction tech-

nique by heating a precursor pellet of $\text{Ba}_2\text{Ca}_{n-1}\text{Cu}_n\text{O}_x$ (not a compound) and a composite Hg source together in an evacuated quartz tube. The precursor pellets were prepared by heating and drying an aqueous solution of appropriate amounts of $\text{Ba}(\text{NO}_3)_2$, $\text{Ca}(\text{NO}_3)_2 \cdot 4\text{H}_2\text{O}$ and $\text{Cu}(\text{NO}_3)_2 \cdot 3\text{H}_2\text{O}$ up to 620°C in a beaker. The resulting black mixture was then ground, compacted, and sintered in flowing oxygen at 900°C for 24 to 48 h in an alumina crucible. These precursor pellets were pulverized, thoroughly mixed with HgO, and compacted (in a glove bag) to form the composite Hg source (prereacted $\text{HgBa}_2\text{Ca}_{n-1}\text{Cu}_n\text{O}_x$). A small precursor pellet and a large composite Hg source (in a ratio of $\sim \frac{1}{3}$) were sealed in an evacuated quartz tube, heated to 810–850°C and kept at this temperature for 3–5 h before cooling to room temperature. The $\text{HgBa}_2\text{Ca}_{n-1}\text{Cu}_n\text{O}_{2n+2+\delta}$ pellets were finally heated at 300°C in flowing oxygen for 10 h.

All the samples were of the highest quality presently available and were obtained from the same synthesis batches as the samples used in high-pressure T_c measurements.¹⁰ Ambient-pressure x-ray diffraction revealed that the samples have a phase purity of $\geq 95\%$ for Hg1201, 90% for Hg1212, and $\sim 80\%$ for Hg1223. Direct-current magnetic susceptibility (χ) results showed superconducting volume fractions consistent with the x-ray data. The nonsuperconducting phases consisted primarily of a ceramic mixture of CaMgO_2 , $\text{Ba}_2\text{Cu}_3\text{O}_{5.9}$, and BaCuO_2 , which bound the ~ 1 – 5 μm superconducting crystallites into brittle pellets. In an attempt to ensure random orientation of the polycrystalline samples we crushed, mixed, and compacted the samples between a diamond and a glass plate, repeating the process four times for each sample. The resulting specimen was a platelet ~ 10 – 20 μm thick with a planar area of 2500–10 000 μm^2 .

High pressure was generated in three separate diamond-anvil cells employing $\frac{1}{3}$ carat diamond anvils with 400–600 μm central flats. The specimen was placed along with a small ruby chip into a 200- μm diam hole in a preindented 60- μm -thick stainless-steel gasket. The sample chamber was filled with neon at 0.2 GPa and sealed between the two diamond anvils. Fluid neon is rigorously hydrostatic up to 5 GPa above which it freezes into a soft quasihydrostatic pressure medium. Pressure was determined by the ruby-fluorescence method¹³ and was measured both before and after data collection to ensure that the pressure was stable. All measurements were performed at 300 K.

The energy-dispersive x-ray-diffraction patterns at fixed angle were collected on the superconducting-wiggler beamline X17c at the National Synchrotron Light Source, Brookhaven National Laboratory. We used an intrinsic-germanium solid-state detector calibrated with several metal-foil fluorescence standards excited by an Americium source. The fixed scattering angle, 2θ , was measured using diffraction from ambient-pressure gold foil. For all measurements reported here 2θ was 13.006° except for the ambient pressure Hg1223 sample which was obtained at 15.040°. Diffraction peaks agreed well with powder-diffraction patterns of the tetragonal unit cell reported for ambient pressure samples.¹⁴ Clear distinction between peaks due to diffraction from the sample and diffraction from the highly compressible neon pressure medium¹⁵ as well as atomic fluorescence lines was achieved by observing the pressure dependence of individual peaks.

The atomic structure of the Hg superconductors consists of rock-salt-type $(\text{BaO})(\text{HgO}_8)(\text{BaO})$ layers alternating with perovskite-type $(n-1)\{(\text{CuO}_2)\text{Ca}\}(\text{CuO}_2)$ layers that form a tetragonal unit cell as shown in Fig. 1.^{16–18} Representative diffraction spectra near 15 GPa are shown in Fig. 2 where we have labeled the tetragonal index assignments that were found to be valid at all pressures for all of our samples. Also noted in Fig. 2 are diffraction lines due to neon,¹⁵ and several impurity lines, as well as the Hg fluorescence lines that dominated the pattern. All three samples reached maximum pressures of ~ 30 GPa.

The Hg1201 and Hg1212 samples were cycled back to ambient pressure showing no hysteresis in the cell parameters, whereas the Hg1223 sample was lost at the highest pressure and the downstroke pressure cycle was not obtained.

Figure 3 shows the pressure dependence of the unit-cell parameters and volume for each sample. All the parameters have been normalized to ambient pressure values to facilitate comparison between samples. Between 6 and 15 diffraction peaks (depending on interference from Hg fluorescence or neon diffraction lines) were used at each pressure to determine the a and c cell parameters by a least-squares fitting routine for each sample. The error bars shown in Fig. 3 correspond to one standard derivation (1σ) uncertainty in the fitted cell parameters. Hg1201 is the most compressible sample in all directions, and the c axis is more compressible than the a axis for all samples. The initial compressions of the a axis and the c axis for Hg1212 and Hg1223 are approximately equal. Above 10 GPa however, Hg1212 is more compressible in the a direction, while Hg1223 is more compressible in the c direction. These asymmetries in the compression of Hg1212 and Hg1223 nearly offset each other, so that their relative volume compressions are almost equal. We measured no difference in the unit-cell parameters with increasing and decreasing pressure.

In order to extract ambient-pressure compressibilities and analytic equations of state we fit the volume data as well as the a and c cell parameters for all three samples to the Murnaghan equation of state,

$$\frac{X}{X_0} = \left[1 + \frac{K'_X}{K_X} P \right]^{-1/K'_X},$$

where X represents either V , a , or c , K_X is the bulk or the elastic modulus, $K_X \equiv -X\partial P/\partial X$, K'_X is the pressure derivative of the elastic modulus, and the subscript 0 refers to ambient-pressure values. The simple Murnaghan equation of state, derived by integrating an assumed linear pressure dependence of K_X , $K_X(P) = K_X + K'_X P$, is sufficient to describe our data.

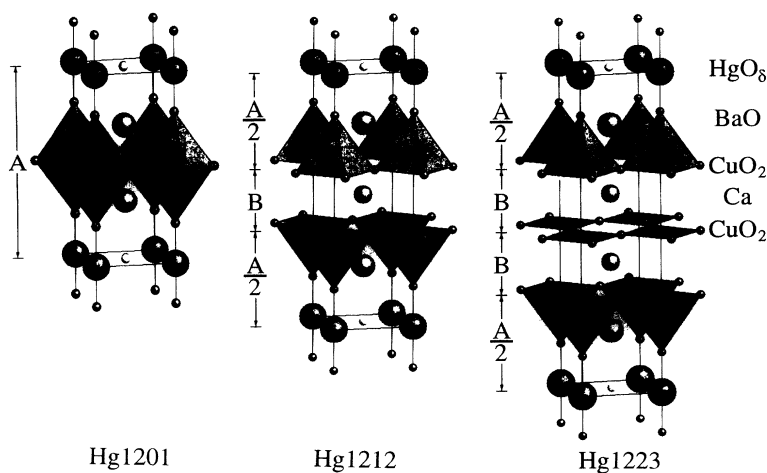


FIG. 1. Crystal structures of the $\text{HgBa}_2\text{Ca}_{n-1}\text{Cu}_n\text{O}_{2n+2+\delta}$ superconductors. $A = 9.50 \text{ \AA}$ and $B = 3.15 \text{ \AA}$ are the distances relating the c -unit-cell dimension at ambient pressure, $c = A + B(n-1)$.

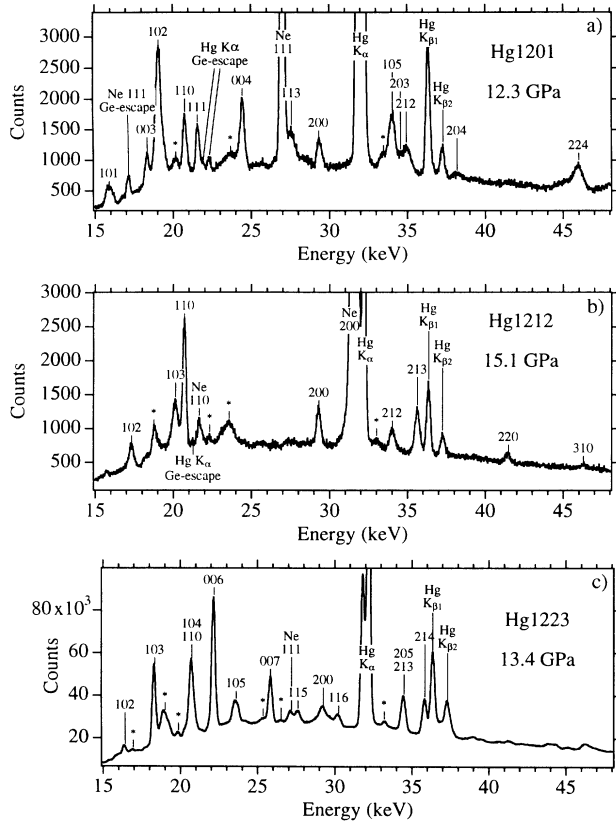


FIG. 2. Energy-dispersive diffraction patterns for the Hg superconductors. The tetragonal indexing is shown for each peak used in our fits. Also marked are the Hg $K\alpha$ and Hg $K\beta$ fluorescence lines, Neon diffraction peaks, intrinsic-germanium-detector escape-peaks and impurity diffraction peaks (*). (a) Hg1201, (b) Hg1212, (c) Hg1223.

We fit our measurements for V , a , and c by a $1/\sigma^2$ -weighted nonlinear-least-squares algorithm, varying the three ambient-pressure parameters in each fit. The lines in Fig. 3 represent the Murnaghan-equation fits to the data. The fitted results for V_0 , a_0 , and c_0 are noted in the figure as well.

While the parameter X_0 is relatively independent of K_{X_0} and K'_{X_0} , a common problem in determining equation of states by high-pressure x-ray diffraction is the interdependence of K_{X_0} and K'_{X_0} . For this reason different assumptions or fitting techniques can lead to large differences in reported values and the most accurate determinations of ambient-pressure moduli are obtained from precise low-pressure measurements. High-pressure data is often fit by holding K_{X_0} fixed at a value determined by ultrasonic data, however this data does not yet exist for these materials. Thus, we report best-fit values in Table I as well as 1σ error ellipses for K_{X_0} and K'_{X_0} calculated from the covariance matrices associated with our weighted, nonlinear fits shown in Fig. 4.¹⁹

The strong interdependence of K_{X_0} and K'_{X_0} is quite obvious in Fig. 4. If one were to artificially constrain either K_{X_0} or K'_{X_0} to a specific value, the best-fit value for

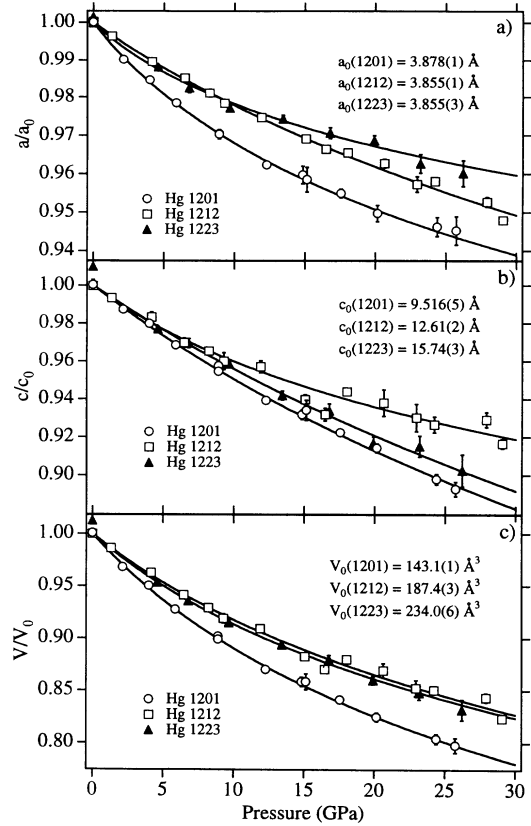


FIG. 3. Determinations of a/a_0 , c/c_0 , and V/V_0 versus pressure based on a tetragonal unit cell. The error bars correspond to 1σ uncertainties. The lines represent weighted-least-squares fits to Murnaghan equations as discussed in the text.

the other parameter would follow the major axes of the error ellipses, plotted as solid lines in Fig. 4. The relative ordering of the major axes allows comparison of the corresponding compression of two samples at high pressure, for example the a axis of Hg1212 is more compressed at high pressure than it is for Hg1223 even though the ambient-pressure elastic moduli suggest the reverse. The strange behavior of the interplane and intraplane compressibilities for Hg1212 and Hg1223 discussed above exhibit themselves as very large K'_{c_0} and K'_{a_0} , respectively.

We have tested the validity of our determinations of the ambient-pressure moduli by fitting our compression data to various three-parameter equations of state, including the Tait equation,²⁰

$$X/X_0 = 1 - \frac{2P}{2K_{X_0} + P(K'_{X_0} + 1)};$$

the Freund-Ingalls equation,²⁰

$$X/X_0 = \left[1 - \frac{1}{jK'_{X_0} + 1} \ln \left(1 + \frac{jK'_{X_0} + 1}{jK_{X_0}} \right) \right]^j;$$

the Birch-Murnaghan equation,²¹

TABLE I. Best-fit parameters of the weighted-least-squares fits to Murnaghan equations. The uncertainties shown in parentheses correspond to one standard deviation. For K_{X_0} and K'_{X_0} the uncertainties include the entire extent of the 1σ error ellipses.

	a_0 (Å)	K_{a_0} (GPa)	K'_{a_0}	c_0 (Å)	K_{c_0} (GPa)	K'_{c_0}	V_0 (Å ³)	K_{V_0} (GPa)	K'_{V_0}
Hg1201	3.8778(14)	201(14)	24.3(26)	9.5160(51)	173(9)	4.9(11)	143.07(13)	65.4(30)	4.53(50)
Hg1212	3.8550(6)	370(14)	15.9(15)	12.609(17)	177(20)	14.8(25)	187.39(25)	91.6(47)	5.30(51)
Hg1223	3.8545(30)	279(25)	40.9(89)	15.742(32)	199(31)	4.6(34)	233.95(61)	83.8(105)	5.8(14)

$$P = \frac{j}{2} K_{X_0} [(X/X_0)^{-7/j} - (X/X_0)^{-5/j}]$$

$$\times \left\{ 1 + \frac{3}{4} \left[\frac{jK'_{X_0}}{3} - 4 \right] [(X/X_0)^{-2/j} - 1] \right\};$$

and the Vinet equation,^{22,23}

$$P = jK_{X_0} (X/X_0)^{-2/j} [1 - (X/X_0)^{1/j}]$$

$$\times \exp \left\{ \frac{3}{2} \left[\frac{K'_{X_0}}{j} - 1 \right] [1 - (X/X_0)^{1/j}] \right\}.$$

In the Freund-Ingalls, the Birch-Murnaghan, and the Vinet equations we have modified the forms slightly to account for the dimensionality of V , a , and c using the parameter

$$j \equiv \begin{cases} 3, & \text{for } V \\ 1, & \text{for } a \text{ and } c. \end{cases}$$

Employing the same $1/\sigma^2$ -weighted nonlinear-least-squares algorithm used for the Murnaghan equation above, each of these equations also gives a reasonable representation of our data. The values obtained for the moduli and their derivatives by fitting our data to these expressions are shown by the hollow symbols in Fig. 4. Clearly, the error ellipses calculated from the Murnaghan fits encompass the values of the moduli obtained from these alternative equations, however the pressure derivatives extend beyond the Murnaghan errors. Thus, we believe that the ambient-pressure moduli reported in Table I are valid to within our quoted uncertainties (obtained from the Murnaghan error-ellipses). We are less confident of the actual values of the pressure derivatives which are strongly dependent on the particular equation employed.

A prediction for the anisotropic compressibilities, κ , of the Hg superconductors using a simple anisotropic-bond model²⁴ has suggested that these superconductors would be very compressible. For comparison, we have shown the predicted moduli ($K \equiv 1/\kappa$) in Fig. 4. Since pressure derivatives of the compressibilities were not calculated, we have displayed the predicted moduli as horizontal dotted lines. It is seen that the K_{a_0} are in fair agreement with our experiment, although the ordering differs for Hg1212 and Hg1223. In contrast, the K_{c_0} are overestimated and the ordering is reversed. Similarly, the ordering of the predictions for the K_{V_0} is seen to differ from experiment, with all the samples being more compressible than predicted. The superiority of predictions for K_{a_0} over K_{c_0} was found previously²⁵ for a large number of high-temperature superconductors.

While the volume compressibilities were underestimated, the model²⁴ successfully predicted the high compressibility of the Hg superconductors with respect to most other high-temperature superconductors. Of the 18 high- T_c superconductors with measured bulk moduli tabulated by Cornelius and co-workers^{24,25} only three have bulk moduli under 100 GPa: $\text{Ti}_2\text{Ba}_2\text{CuO}_{6+\delta}$, $\text{Bi}_2\text{Sr}_2\text{CaCu}_2\text{O}_8$, and $\text{Bi}_{1.9}\text{Pb}_{0.3}\text{Sr}_2\text{Ca}_{1.9}\text{Cu}_3\text{O}_{10.25}$ with $K_{V_0} = 82, 61$, and 73 GPa, respectively. In the model cal-

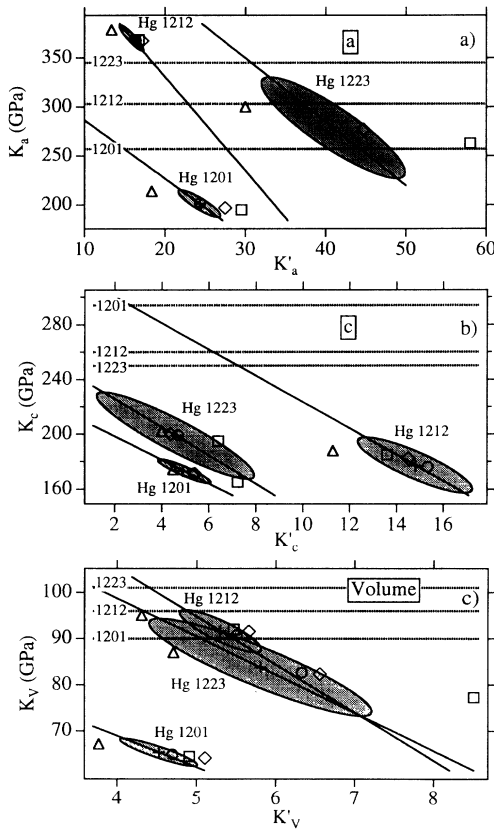


FIG. 4. Bulk and elastic moduli vs their pressure derivatives. The shaded areas correspond to 1σ error ellipses corresponding to the weighted-least-squares fits to Murnaghan equations as discussed in the text. The dotted lines represent model theoretical predictions of the moduli (Ref. 24) (no pressure derivatives were calculated). The pluses correspond to values fit to a Murnaghan equation, the triangles to a Tait equation, the circles to a Freund-Ingalls equation, the squares to a Birch-Murnaghan equation, and the diamonds to a Vinet equation as discussed in the text.

culation the $(\text{BaO})(\text{HgO}_8)(\text{BaO})$ layers lead to this high compressibility.

We tried to experimentally test the relative compressibility of the $(\text{BaO})(\text{HgO}_8)(\text{BaO})$ and the $(n-1)\{(\text{CuO}_2)\text{Ca}\}(\text{CuO}_2)$ layers by comparing the compression data for different samples. At ambient pressure c is well represented by the relation $c = A + B(n-1)$, with $A = 9.50 \text{ \AA}$ and $B = 3.15 \text{ \AA}$, up to $n = 4$ and probably $n = 5$.²⁶ If this relation continues to hold at high pressure, we could examine the relative compressibilities of the individual layers by finding the pressure dependences of A [due to the $(\text{BaO})(\text{HgO}_8)(\text{BaO})$ layers] and B [due to the $(n-1)\{(\text{CuO}_2)\text{Ca}\}(\text{CuO}_2)$ layers]. Unfortunately, this linear relation fails to hold at pressures above about 10 GPa as shown in Fig. 5. This breakdown may occur because, unlike Hg1201 and Hg1223, Hg1212 does not have a CuO_2 layer on a mirror plane which may reduce its compressibility in the c direction. The nonlinear relation at high pressure results from the strange relationship among a and c compression noted above for Hg1212 and Hg1223. One implication of this result is that a crucial assumption of the simple anisotropic-bond model,²⁵ the additivity of layer compressibilities, breaks down above 10 GPa in the Hg superconductors.

We have measured the compressibilities of the new Hg superconductors in a diamond-anvil cell using energy-dispersive synchrotron x-ray diffraction. We report the tetragonal cell parameters a and c up to 30 GPa. We have extrapolated zero-pressure bulk moduli of 65.4(3.0), 91.6(4.2), and 83.8(10.5) GPa for Hg1201, Hg1212, and Hg1223, respectively. The Hg superconductors have high compressibilities compared to other high-temperature superconductors which generally show bulk moduli in the range of 100–200 GPa. For Hg1212 and Hg1223, differences in the pressure dependences of the inter- and intralayer compressions largely offset so that the bulk compressibilities are quite similar. Finally, the

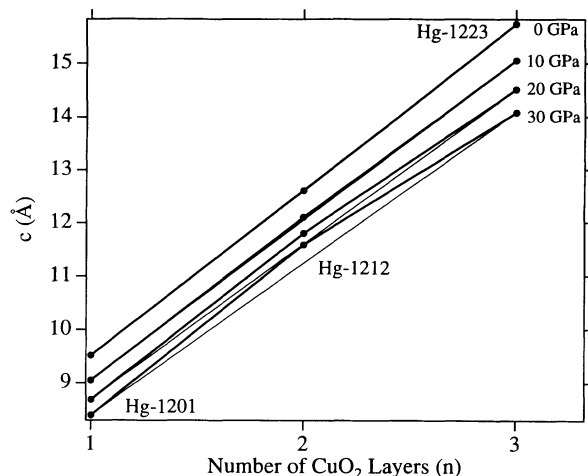


FIG. 5. Values of c plotted against n at various pressures. Above about 10 GPa c is no longer linear with n , as shown by the thin lines drawn through the points for Hg1201 and Hg1223.

relation $c = A + B(n-1)$ holds for the c -axis cell parameter at ambient pressure, however the relation breaks down at high pressures.

We thank B. Downs, L. Finger, M. Hanfland, and W. Vos for useful discussions. We thank Kurt Bartelmehs and Bob Downs for access to a demo version of their program XTALDRAW. Work at Washington, D.C. was supported by the National Science Foundation and the Carnegie Institution of Washington. Work at Houston was supported in part by NSF Grant No. DMR 91-22043, USAFOSR Grant No. F49620-93-1-0310, BMDO, ARPA Grant No. MDA 972-90-J-1001, the State of Texas through the Texas Center for Superconductivity at the University of Houston, and the T. L. L. Temple Foundation.

¹S. N. Putilin, E. V. Antipov, O. Chmaissem, and M. Marezio, *Nature* (London) **362**, 226 (1993).

²Z. J. Huang, R. L. Meng, X. D. Qiu, Y. Y. Sun, J. Kulik, Y. Y. Xue, and C. W. Chu, *Physica C* **217**, 1 (1993).

³L. Gao, Z. J. Huang, R. L. Meng, J. G. Lin, F. Chen, L. Beauvais, Y. Y. Sun, Y. Y. Xue, and C. W. Chu, *Physica C* **213**, 261 (1993).

⁴A. K. Klehe, A. K. Gangopadhyay, J. Diederichs, and J. S. Schilling, *Physica C* **213**, 266 (1993).

⁵F. Chen, Z. J. Huang, R. L. Meng, Y. Y. Sun, and C. W. Chu, *Phys. Rev. B* **48**, 16047 (1993).

⁶F. Chen, L. Gao, R. L. Meng, Y. Y. Xue, and C. W. Chu (unpublished).

⁷L. Gao, F. Chen, R. L. Meng, Y. Y. Xue, and C. W. Chu, *Philos. Mag. Lett.* **68**, 345 (1993).

⁸C. W. Chu, L. Gao, F. Chen, Z. J. Huang, R. L. Meng, and Y. Y. Xue, *Nature* (London) **365**, 323 (1993).

⁹M. Nunez-Regueiro, J. L. Tholence, E. V. Antipov, J. J. Capponi, and M. Marezio, *Science* **262**, 97 (1993).

¹⁰L. Gao, Y. Y. Xue, F. Chen, Q. Xiong, R. L. Meng, D. Ramirez, C. W. Chu, J. H. Eggert, and H. K. Mao (unpublished).

lished).

¹¹W. H. Fietz, H. A. Ludwig, B. P. Wagner, K. Grube, R. Benischke, and H. Wuhl, *Elastic Properties of High Temperature Superconductors Derived From High Pressure Experiments* (Plenum, New York, 1991), p. 433.

¹²R. L. Meng, L. Beauvais, X. N. Zhang, Z. J. Huang, Y. Y. Sun, Y. Y. Xue, and X. W. Chu, *Physica C* **216**, 21 (1993).

¹³H. K. Mao, J. Xu, and P. M. Bell, *J. Geophys. Res.* **91**, 4673 (1986).

¹⁴Y. T. Ren, H. Chang, Q. Xiong, Y. Q. Wang, Y. Y. Sun, R. L. Meng, Y. Y. Xue, and C. W. Chu, *Physica C* **217**, 273 (1993).

¹⁵R. J. Hemley, C. S. Zha, A. P. Jephcoat, H. K. Mao, and L. W. Finger, *Phys. Rev. B* **39**, 11 820 (1989).

¹⁶J. L. Wagner, P. G. Radaelli, D. G. Hinks, J. D. Jorgensen, J. F. Mitchell, B. Dabrowski, G. S. Knapp, and M. A. Beno, *Physica C* **210**, 447 (1993).

¹⁷Q. Huang, J. W. Lynn, R. L. Meng, and C. W. Chu, *Physica C* **218**, 356 (1993).

¹⁸O. Chmaissem, Q. Huang, E. V. Antipov, S. N. Putilin, M. Marezio, S. M. Loureiro, J. J. Capponi, J. L. Tholence, and A. Santoro, *Physica C* **217**, 265 (1993).

- ¹⁹H. W. Press, B. P. Flannery, S. A. Teukolsky, and W. T. Vetterling, *Numerical Recipes* (Cambridge University Press, Cambridge, 1989), p. 529.
- ²⁰J. Freund and R. Ingalls, *J. Phys. Chem. Solids* **50**, 263 (1989).
- ²¹R. G. Munro, S. Block, and G. J. Piermarini, *J. Appl. Phys.* **56**, 2174 (1984).
- ²²P. Vinet, J. Ferrante, J. R. Smith, and J. H. Rose, *J. Phys. C* **19**, L467 (1986).
- ²³P. Vinet, J. Ferrante, J. H. Rose, and J. R. Smith, *J. Geophys. Res.* **92**, 9319 (1987).
- ²⁴A. L. Cornelius and J. S. Schilling, *Physica C* **218**, 369 (1993).
- ²⁵A. L. Cornelius, S. Klotz, and J. S. Schilling, *Physica C* **197**, 209 (1992).
- ²⁶E. V. Antipov, S. M. Loureiro, C. Chaillout, J. J. Capponi, P. Bordet, J. L. Tholence, S. N. Putilin, and M. Marezio, *Physica C* **215**, 1 (1993).

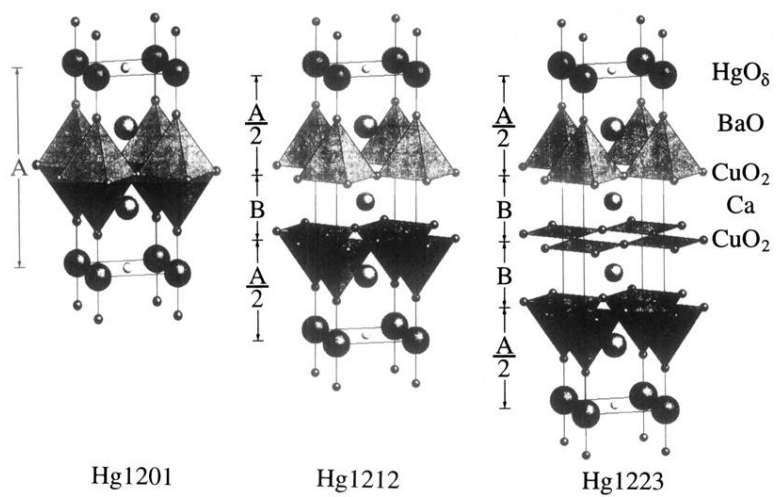


FIG. 1. Crystal structures of the $\text{HgBa}_2\text{Ca}_{n-1}\text{Cu}_n\text{O}_{2n+2+\delta}$ superconductors. $A = 9.50 \text{ \AA}$ and $B = 3.15 \text{ \AA}$ are the distances relating the c -unit-cell dimension at ambient pressure, $c = A + B(n - 1)$.

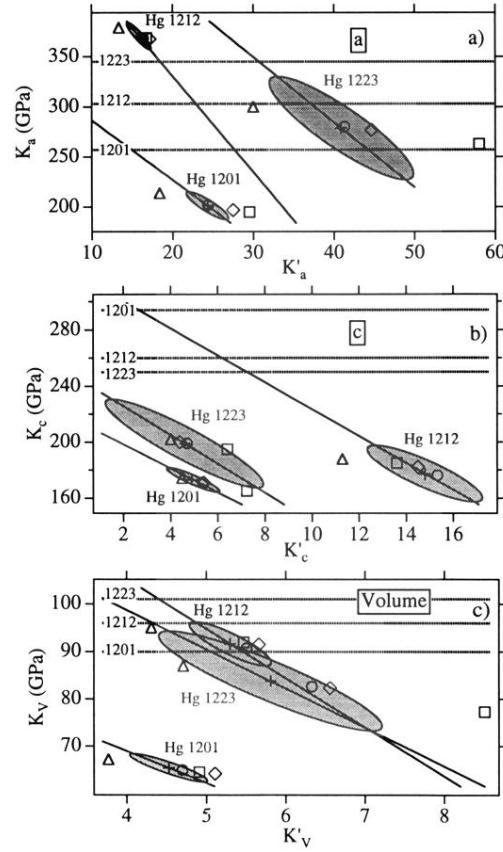


FIG. 4. Bulk and elastic moduli vs their pressure derivatives. The shaded areas correspond to 1σ error ellipses corresponding to the weighted-least-squares fits to Murnaghan equations as discussed in the text. The dotted lines represent model theoretical predictions of the moduli (Ref. 24) (no pressure derivatives were calculated). The plusses correspond to values fit to a Murnaghan equation, the triangles to a Tait equation, the circles to a Freund-Ingalls equation, the squares to a Birch-Murnaghan equation, and the diamonds to a Vinet equation as discussed in the text.